Effect of Hydrodynamic Interactions on the Diffusion of Integral Membrane Proteins: Tracer Diffusion in Organelle and Reconstituted Membranes

Stuart J. Bussell, Donald L. Koch, and Daniel A. Hammer
School of Chemical Engineering, Cornell University, Ithaca, New York 14853 USA

ABSTRACT A persistent discrepancy exists between theoretical predictions and experimental observations for the diffusion coefficients of integral membrane proteins in lipid bilayers free of immobilized proteins. Current thermodynamic theories overestimate tracer diffusion coefficients at high area fractions. We explore the hypothesis that the combined effect of hydrodynamic and thermodynamic interactions reconciles theory with experiment. We have determined previously the short- and long-time tracer diffusivities, D_s and D_l, respectively, of integral membrane proteins in lipid bilayers as a function of their area fraction, ϕ. The results are based on two-particle hydrodynamic and thermodynamic interactions and are precise to $O(\phi)$. Here we extend the results for D_l to high ϕ by combining the hydrodynamic results for D_s into theories for D_l based on many-particle thermodynamic interactions. The results compare favorably with the experimental measurements of D_l as a function of protein area fraction for bacteriorhodopsin in reconstituted membranes and for complex III of the mitochondrial inner membrane. The agreement suggests that both hydrodynamic and thermodynamic interactions are important determinants of diffusion coefficients of proteins in lipid bilayers. Additional experiments are required to verify the role of hydrodynamic interactions in protein diffusion in reconstituted systems.

INTRODUCTION

Eukaryotic membranes are principally suspensions of integral membrane proteins (IMPs) in fluid lipid bilayers (Singer and Nicolson, 1972). Proteins and lipids combined compose by weight the vast majority of plasma and organelle membranes (Gennis, 1989). Biological membranes can be categorized based on the presence or absence of immobilized protein. Typically, only 70% of the IMPs in plasma membranes are mobile, whereas nearly 100% are mobile in the membranes of organelles (Edidin, 1987). Immobilization is thought to occur when the cytoplasmic tails of IMPs interact with cytoskeletal elements underlying the plasma membrane (Tank et al., 1982; Wu et al., 1982; Henis and Elson, 1981). As a result of the immobilization, the protein dynamics in plasma membranes tend to be slower than the dynamics in organelle membranes. For instance, translational diffusivities can be one to several orders of magnitude slower in plasma membranes than in organelle or reconstituted membranes (Edidin, 1987).

Artificial bilayers reconstituted with IMPs are simple systems of well defined composition that can be used for the study of the dynamics of IMPs. Because they lack cytoskeletal components, their dynamics resemble those of organelle membranes. In this paper, we are interested in protein diffusion in organelle and reconstituted membranes, hereafter referred to as lipid bilayers. In the companion paper (Bussell et al., 1995), we address the diffusivity of proteins in plasma membranes.

A commonly used technique for measuring tracer diffusion coefficients of IMPs is fluorescent photobleaching and recovery (FPR) (Axelrod et al., 1976). The IMPs are labeled with a fluorescent probe, and a small fraction of the total area of the membrane is exposed to a focused, high intensity laser beam. In the area of illumination, the fluorophores are bleached. Then the laser beam is attenuated to a power sufficient to excite the fluorophores with negligible bleaching, and the increase in fluorescence emission from the previously bleached spot, resulting from the diffusion of unbleached IMPs into that region, can be used to determine the diffusivity and mobility of the labeled proteins.

Experiments have shown that tracer diffusion coefficients of IMPs in multilamellar lipid bilayer vesicles decrease as the area fraction of proteins, ϕ, increases (Peters and Cherry, 1982; Chazotte and Hackenbrock, 1988). Diffusion coefficients of bacteriorhodopsin reconstituted in artificial bilayers were measured for lipid/protein molar ratios, *LP*, from 30 to 210 (Peters and Cherry, 1982). The virtue of these measurements is the simple composition of the experimental system. In contrast to in vivo systems, the reconstituted system used in these experiments contained only a single species of both protein and lipid. The diffusion coefficients of bacteriorhodopsin decrease as *LP* decreases (ϕ increases).

Chazotte and Hackenbrock (1988) measured diffusion coefficients of complex III of the mitochondrial electron transport chain in inner mitochondrial membranes. They varied protein concentrations by incorporating exogenous soybean phospholipid into the inner membranes. They presented their data in terms of a lipid enrichment factor, *LE*, defined as the ratio of the mass of lipid in the membrane after soybean

Received for publication 12 November 1992 and in final form 23 January 1995.

Address reprint requests to Dr. Hammer, School of Chemical Engineering, Cornell University, Ithaca, NY 14853. Tel.: 716-275-2482; Fax: 716-275-6007; E-mail: hammer@cheme.tn.cornell.edu.

Dr. Bussell's present address: PRIZM Pharmaceuticals, 11035 Roselle St., San Diego, CA 92121.

0006-3495/95/05/1828/08 $2.00

phospholipid addition to the mass of lipid in the membrane before addition. In their experiments, *LE* varied from 1 to 8. Lower values of *LE* correspond to higher IMP area fractions. Again, diffusion coefficients decrease as ϕ increases. Because endogenous mitochondria were used as a starting point for the lipid dilution, the composition of the lipids and IMPs in this system remained highly heterogeneous.

Previous theoretical explanations of the experimental data from these studies did not consider hydrodynamic interactions between proteins because, until recently, no one had correctly solved for these interactions (Scalettar and Abney, 1991). Pink (1985) and Saxton (1987) performed Monte Carlo computer simulations to explore the effect of protein area fraction on the diffusivity of IMPs. They ignored hydrodynamic interactions and concentrated on interparticle potential energy interactions. Abney et al., (1989a, 1989b) used a semi-analytic technique to correlate protein diffusivities to area fractions for a particle undergoing both tracer and gradient diffusion. They also ignored hydrodynamic interactions but retained three-body thermodynamic interactions, and their results for tracer diffusion coefficients coincide remarkably well with the results from Monte Carlo simulations for the effect of protein area fraction on protein diffusivity. However, both simulations and semi-analytic theories fail to fit accurately the experimental observations (Saxton, 1987; Scalettar and Abney, 1991). Specifically, the theoretical predictions overestimate tracer diffusivities at all but the lowest protein area fractions, and the discrepancy is greatest at the highest area fractions. A potential explanation for the discrepancy between theory and experiment is that hydrodynamic interactions were excluded from these studies.

To understand the role of hydrodynamics in protein diffusion in lipid membranes, we use techniques from suspension mechanics that have been quite useful in elucidating the diffusive behavior of spheres in three-dimensional suspensions (Medina-Noyala, 1988; Russel and Gast, 1986). Biological membranes can be thought of as analogous two-dimensional suspensions of proteins in lipid fluid. We recognize that there are two characteristic tracer diffusion coefficients for IMPs that differ according to their time scale. The short-time tracer diffusion coefficient of an IMP is valid for times $t \sim t_s \ll a^2/D$, where a is its radius in the membrane, D is its scalar diffusivity, and t_s is the shortest time for which a diffusivity can be described. (The exact value of t_s is a subject of some debate, both in two- and three-dimensional suspensions, depending on whether inertial or purely viscous fluid effects are important. The exact value of t_s is not important for this analysis). The time scale, a^2/D, is the time required for the particles to travel a distance comparable with a. For $a = 2$ nm and $D = O(10^{-9}$ cm^2/s), $a^2/D = O(10^{-4}$ s). For times much less than a^2/D, the structure of the suspension relative to the particle positions remains nearly unchanged. Diffusion coefficients for $t \sim t_s \ll a^2/D$ are short-time coefficients, D_s, and they are solely determined by hydrodynamic effects and independent of excluded area effects between IMPs. In contrast, for $t \gg a^2/D$, motions of tracer particles are influenced by interparticle and excluded area interactions. Because excluded area effects inhibit diffusive motion, long-time diffusion coefficients are less than D_s. As t goes from t_s to a time much greater than a^2/D, D decreases steadily until it reaches its steady long-time value, D_l. All previously cited experiments have attempted to measure D_l.

Our goal is to determine the effect of hydrodynamic interactions on D_l at high ϕ and compare the results with experiment. We have previously calculated D_s and D_l based on two-particle hydrodynamic and thermodynamic interactions (Bussell et al., 1992, 1994). In this paper, we extend these results to high ϕ by combining the results for D_s based on hydrodynamic interactions with the results for D_l obtained by methods that ignore hydrodynamic interactions but include many-particle excluded area effects.

As mentioned earlier, hydrodynamic interactions are the sole determinant of D_s. In contrast, according to Rallison (1988), the strongest determinant of D_l/D_s is the hindered motion of the particles due to thermodynamic interactions. Therefore, we assume hydrodynamics have a small effect on D_l/D_s and can be neglected to estimate its value. We reconcile these two views and use both the hydrodynamic results for D_s and the multibody thermodynamic results for D_l/D_s to calculate a physically consistent D_l. Comparison of the results with experimental data for bacteriorhodopsin and mitochondrial complex III shows that the experimental observations can be explained successfully with a combined hydrodynamic-thermodynamic approach.

THEORY

Short-time tracer diffusion coefficients

Short-time diffusion coefficients are only affected by hydrodynamic interactions that operate on the time scale $t \ll a^2/D$. Saffman and Delbruck (1975) used a model of the membrane lipid as a continuum fluid to calculate the mobility of a single protein in a biological membrane of infinite extent. Strictly, the continuum approximation would be satisfied when the ratio of lipid to protein radius is much smaller than one. In reality, the ratio of lipid to protein radius is between some fraction of one (perhaps as small as 0.1) to one, and Saffman and Delbruck (1975) assumed the continuum approximation would be valid over much of this range. At infinite dilution, both short- and long-time diffusion coefficients for IMPs are given by (Saffman and Delbruck, 1975):

$$D_0 = \frac{k_b T}{4\pi\mu h}[\ln(\lambda) - \gamma]. \quad (1)$$

Here, $\lambda = \mu h/\mu' a$, where h is the membrane thickness, a is the protein radius, μ and μ' are the viscosities of the membrane and surrounding aqueous phases, respectively, and γ is Euler's constant. Because Eq. 1 properly describes protein diffusion at infinite dilution (Scalettar and Abney, 1991), the continuum approximation is likely valid for some protein-membrane systems, but it will be most appropriate for small ratios of lipid/protein radii.

For time scales $t \ll a^2/D_0$ and $\phi > 0$, hydrodynamic interactions between IMPs reduce D_s from the infinite dilution limit, D_0, given by (1). The leading order effects of hydrodynamic interactions occur between two-particle interactions. Results for the two-particle interactions (Bussell et al., 1992) have been used recently to calculate D_s to leading order in ϕ (Bussell et al., 1994). The calculations for D_s ensemble average the two-particle interactions, and the results depend on λ. To $O(\phi/\ln(\lambda))$ they are

$$\frac{D_s}{D_0} = 1 - 2\phi\left[1 - \frac{1 + \ln(2) - 9/32}{\ln(\lambda) - \gamma}\right]. \quad (2)$$

D_s differs significantly from D_0 at nonzero IMP area fractions.

The result in (2) for D_s/D_0 depends on both ϕ and λ, although the functional dependence on ϕ is much stronger. As a result, theoretical predictions for IMP diffusion coefficients are significantly more sensitive to parameters affecting ϕ.

Long-time tracer diffusion coefficients

Previous work to calculate the long-time tracer diffusivity, D_l, has involved methods such as Monte Carlo simulation (Saxton, 1987), Brownian integral methods (Abney et al., 1989a), or free volume models (Minton, 1989). These techniques are reviewed by Scalettar and Abney (1991). All of these techniques account for the hindered motion of IMPs for $t \gg a^2/D$ and include thermodynamic interactions, but exclude hydrodynamic interactions. In Monte Carlo techniques, the diffusivity calculated in simulation time is related to a diffusivity calculated in real time using a reference diffusivity, D_{ref}. Often, results are expressed as D_l/D_{ref}. The reference diffusivity is the characteristic diffusion coefficient for the smallest excursions or times for which a diffusion coefficient can be defined. When hydrodynamic interactions are excluded, D_{ref} is assumed to be D_0, regardless of ϕ. Strictly, D_{ref} is D_0 only at infinite dilution and, at higher area fractions, the appropriate reference diffusivity is D_s. Therefore, Monte Carlo results give D_l/D_s. The other techniques for determining D_l cited above also provide values for D_l/D_0 when hydrodynamic interactions are excluded, but there are ways of directly incorporating hydrodynamic interactions into these models if the appropriate hydrodynamic functions are known (Russel and Gast, 1986), although this has not yet been done for two-dimensional diffusion (Scalettar and Abney, 1991).

If D_l/D_{ref} is available from thermodynamic methods, and D_s is available from hydrodynamic calculations, the long-time tracer diffusivity can be constructed from the two:

$$D_l = \left(\frac{D_l}{D_{ref}}\right) D_s. \quad (3)$$

This technique has been used in suspension mechanics to calculate long-time diffusivities of spheres in concentrated suspensions (Medina-Noyala, 1988), and the results compare favorably with measured diffusivities. Our aim is to use our calculation of D_s, combined with previously reported calculations of D_l/D_{ref}, calculate D_l using (3), and compare the results with existing data of protein diffusion.

We consider two ways to calculate D_l/D_{ref}. First, Saxton (1987) provides a fit to Monte Carlo results for D_l/D_{ref} as a function of area fraction, ϕ, for hard-core repulsive interactions in systems where all the proteins are mobile. He found (Saxton, 1987):

$$\frac{D_l}{D_{ref}} = 1 - 2.1187\phi + 1.8025\phi^2 - 1.6304\phi^3 + 0.9466\phi^4. \quad (4)$$

The results given by Abney et al., (1989a), using Brownian integral methods, are in basic agreement with Eq. 4. Although Abney et al. (1989a) considered several types of interparticle potentials, we restrict our consideration to hard-core repulsions.

An alternative technique for calculating D_l/D_{ref} is given by Rallison (1988), which we adapt here to diffusive motions in two dimensions. According to Rallison (1988), the effects of the coordinated motions, or "caging," of particles needed for long-time diffusion at high area fractions dominate the effects of hydrodynamic interactions operating on time scales $t \gg a^2/D$. Based on his reasoning, as area fractions become large, techniques that neglect hydrodynamic interactions should be effective at calculating D_l/D_{ref}. Rallison demonstrated the utility of his hypothesis by comparing his theoretical results with both Monte Carlo simulation results and experimental observations from a variety of systems. Therefore, we might expect the results given in (4) to be accurate at high ϕ despite the neglect of hydrodynamic interactions. On the other hand, hydrodynamic interactions should be the principle determinants of diffusivities at low ϕ.

The conjecture that forms the basis for Rallison's technique is that long-time diffusivities are inversely proportional to the number of particles, N, "caging" a tracer particle and related to the time, t_c, required for the tracer particle to escape its cage. The mean-square displacement, $\langle x_0^2 \rangle$, for a particle is a function of time. As $t \to 0$, $\langle x_0^2 \rangle \to 2D_s t$, and as $t \to t_c$, $\langle x_0^2 \rangle \to 2D_l t_c$. Rallison postulates that $\langle x_0^2 \rangle$ for a tracer particle is

$$\langle x_0^2 \rangle(t) = \frac{1}{\pi} \int_0^{(4\pi D_s t)^{1/2}} \frac{\xi d\xi}{N(\xi)}, \quad (5)$$

where $\xi = (4\pi D_s t')^{1/2}$ and t' is a variable of integration. The tracer particle is itself included in N, and the integral in (5) has the correct limit as $t \to 0$. With the proper definitions for N and t_c, (5) can be used to calculate D_l.

The time t_c is related to the distance d_c that a particle must travel to escape its cage and enter a new one. From (5), the relationship is

$$d_c^2 = 2D_l t_c = \frac{1}{\pi} \int_0^{(4\pi D_s t_c)^{1/2}} \frac{\xi d\xi}{N(\xi)}. \quad (6)$$

The values of N and t_c or d_c are determined by following the

progressive motion of a tracer particle. As the tracer advances, all N particles, which are assumed to form a roughly circular region of radius $R(x)$, advance (see Fig. 1). When the tracer advances a rectilinear distance dx, a new particle is contacted and recruited by the advancing front of the cage if its center lies in the area $dA = 2(R + a)dx$. Therefore,

$$\frac{dN}{dx} = n2(R + a), \tag{7}$$

where n is the number density of IMPs. The radius R also increases as the tracer moves if newly contacted particles are on the periphery of the cage. The cage diameter changes according to the equation, $d(2R)$ = (the probability a new disk is hit at the periphery of R) × (expected length of overlap). For all R, the cage increases its radius R if one of its two ends strikes a disk, and this occurs if a particle center lies in the area $2(2a)dx$. The average length of overlap is a, so that

$$\frac{dR}{dx} = 2ana = \frac{2\phi}{\pi}. \tag{8}$$

Equations (7) and (8) yield

$$N(x) = \frac{2\phi^2x^2}{\pi^2a^2} + \frac{6\phi x}{\pi a} + 1. \tag{9}$$

The values of t_c and d_c must be determined before we can calculate D_l/D_{ref}. Rallison advocates the choice of a for d_c, and this choice is appropriate at high ϕ. At high ϕ, when a protein moves a distance a, it likely exits the cage that confines it based on the highly ordered structure of the IMPs at high area fractions. At lower ϕ, caging structures do not exist. There simply are not enough particles to form networks of confining particles. Despite this, we extend the results to low ϕ to generate continuous results, always assuming that $d_c = a$.

If we substitute $d_c = a$ and N from (9) into (6), we find the implicit solution:

$$1 = \frac{\pi}{4\phi^2}\left[\ln\left(\frac{2\phi^2}{\pi^2}\xi^2 + \frac{6\phi}{\pi}\xi + 1\right) - \frac{3\sqrt{7}}{7}\cdot \ln\left[\frac{(3+\sqrt{7})\left(3 + \frac{2\phi}{\pi}\xi - \sqrt{7}\right)}{(3-\sqrt{7})\left(3 + \frac{2\phi}{\pi}\xi + \sqrt{7}\right)}\right]\right],$$

$$\text{where } \xi = \left(\frac{4\pi D_s t_c}{a^2}\right)^{\frac{1}{2}}. \tag{10}$$

We can solve for t_c using a simple root solver. After inserting t_c into (6), we arrive at the solution for D_l/D_{ref}. D_l/D_{ref} decreases monotonically with increasing ϕ, although $D_l/D_{ref} > 0$ over the domain $0 \le \phi \le 1$.

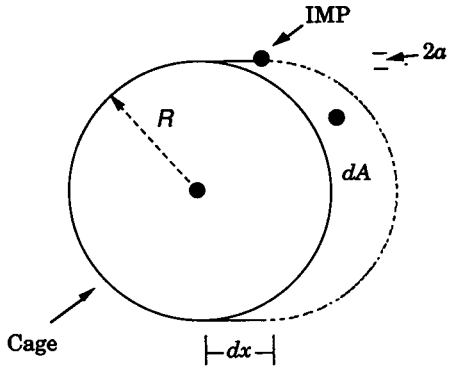

FIGURE 1 The motion of a tracer particle and its cage. R is the radius of the cage, a is the radius of the IMP, dx is the differential distance of translation of the cage, and dA is the differential area change associated with a displacement of dx.

The results for D_l/D_{ref} calculated by Saxton (1987; Eq. 4) and calculated above using the method of Rallison (Eq. 6) are plotted as function of ϕ in Fig. 2. Both of these methods incorporate multiple hard-core interactions and agree closely with each other over the domain of interest, $0 \le \phi \le 0.6$. Based on this comparison, the assumptions that lead to the results based on caging theory seem to be correct. Furthermore, we have two independent methods to determine D_l/D_{ref} that agree quantitatively at physically realistic ϕ.

Using Eq. 3, either of these results for D_l/D_{ref} (Eqs. 4 or 6), valid at all ϕ, can be combined with the result for D_s/D_0 (Eq. 2), valid to $O(\phi/\ln\lambda)$, to construct D_l/D_0 as a function of ϕ. This function will be strictly valid at low ϕ, but may also be valid at higher ϕ if interactions in concentrated suspensions are dominated by thermodynamics at high ϕ, and the low ϕ asymptote is adequate to describe hydrodynamic interactions at higher concentrations. This physical picture would be consistent with the conjecture of Rallison (1988). These result for D_l/D_0 can be compared with an expression derived by Bussell et al. (1994) for D_l/D_0 as a function of ϕ that takes into account two body hydrodynamic and thermodynamic interactions only, and is only valid at low ϕ (Bussell et al., 1994):

$$\frac{D_l}{D_0} = \frac{D_s}{D_0} - \frac{0.07\phi}{\ln(\lambda) - \gamma}, \tag{11}$$

Equation 11 is rigorously valid in the limit of low area fraction and can be considered the low ϕ asymptote for D_l, in contrast to Eq. 2, which is the low ϕ asymptote for D_s.

COMPARISON OF THEORY WITH EXPERIMENT

The theoretical results for D_l/D_0 obtained from combinations of Eqs. 4 and 2 with 3 are plotted in Fig. 3 for $\lambda = 250$ and in Fig. 4 for $\lambda = 750$. In Fig. 3, we also plot two other theoretical curves for comparison. One is D_l/D_{ref} from Eq. 4 calculated by Saxton (1987). The other is the low ϕ asymptote for D_l/D_0 (Eq. 11) where Eq. 2 was used to determine D_s/D_0. We have also included this low ϕ asymptote in Fig. 4. The experimental results for bacteriorhodopsin and complex III are also given in Figs. 3 and 4, respectively.

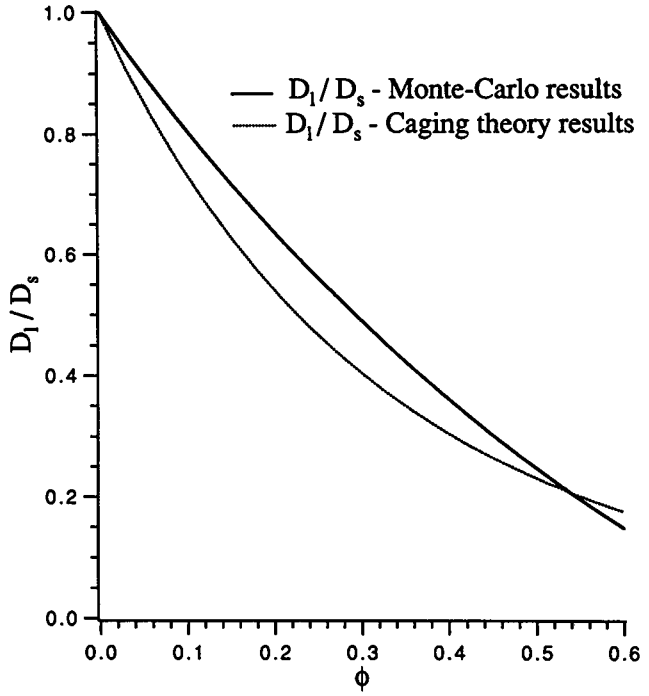

FIGURE 2 Comparison between theoretical results for D_l/D_s based on Monte Carlo simulations (Saxton, 1987) and the caging theory (this work).

Several assumptions have to be made to interpret the experimental data to construct Figs. 3 and 4. The value of λ is set to 250 for the bacteriorhodopsin system based on the approximate values $a = 2$ nm, $\mu = 1$ poise, $h = 5$ nm, and $\mu' = 1$ centipoise (Peters and Cherry, 1982). We use the crystal radii for *both* the protein and lipid for consistency to calculate ϕ. They are approximately $a = 1.75$ nm (Henderson and Unwin, 1975) and $a_l = 0.4$ nm, where a_l is the radius of a typical lipid molecule (Gennis, 1989). Because the lipids form a bilayer and the protein resides almost entirely in the membrane, the area fraction is

$$\phi = \frac{1}{1 + (a_l^2 LP)/(2a^2)}, \tag{12}$$

where LP is the lipid/protein molar ratio.

At the most dilute IMP concentrations, complex III diffuses approximately one-third as quickly as bacteriorhodopsin. This suggests that the viscosity of the inner mitochondrial membrane is approximately 3 times the viscosity of the bilayer used in the bacteriorhodopsin experiments because the Saffman-Delbruck diffusivity varies approximately linearly with membrane viscosity. Therefore, we assume $\lambda = 750$ for this system. Because we have made this determination at the most dilute concentration of protein, we minimize any possible differences between the effective viscosity and the viscosity of the pure lipid. In addition, we have to estimate certain properties of the proteins and lipids in native and enriched mitochondrial inner membranes to convert the original lipid enrichment data to IMP area fractions. The native membrane has a weight ratio of protein to lipid, *pl*, of 4:1 (Gennis, 1989). We assume that the proteins and lipids

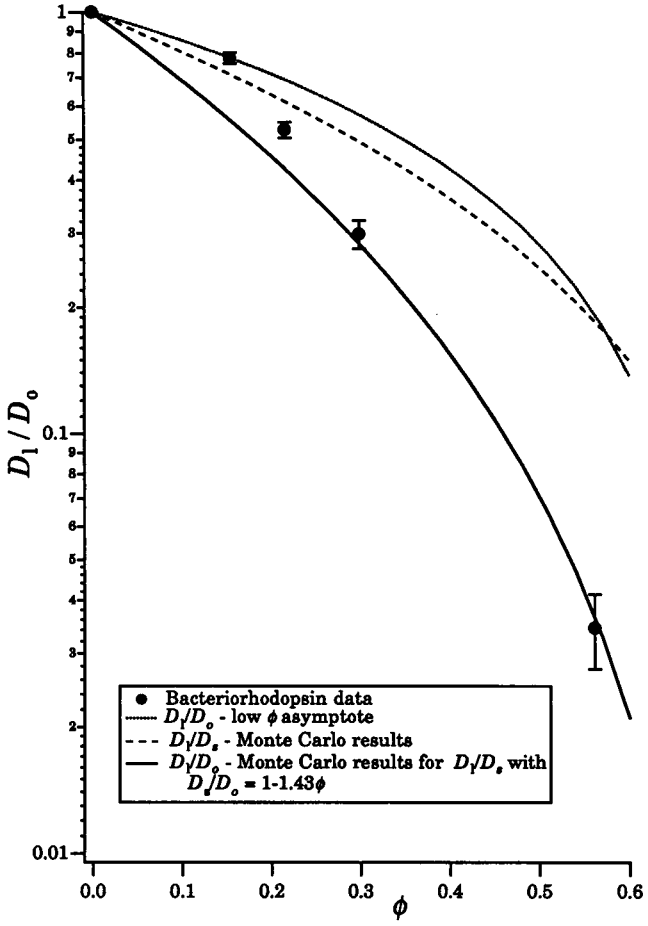

FIGURE 3 Comparison between theory and experiment for the diffusion of bacteriorhodopsin. The theoretical predictions fit the experimental data only when both hydrodynamic and thermodynamic interactions are incorporated into the calculations. Low ϕ results (Eq. 2) and solely thermodynamic results (Saxton, 1987) are shown for comparison. The experimental data and error bars are interpreted from the results at 32°C reported in Table 3 and Fig. 3, respectively, of Peters and Cherry (1982).

have typical densities of $\rho_p = 1.36$ g/ml and $\rho_l = 0.9$ g/ml, respectively. The density of protein is commonly known, and the density of lipid is estimated from average values for lipids—molecular weight equal to 800 g/mole, cross sectional area equal to 60 Å in the plane of the membrane, and height equal to half the membrane thickness, ~25 Å (Gennis, 1989). Furthermore, we assume that the fraction of the IMPs total weight actually residing in the membrane, *PF*, is between 0.3 and 0.4 based on the three-dimensional structures of known mitochondrial IMPs (Deatherage et al., 1982; Leonard et al., 1987). The area fraction is

$$\phi = \frac{1}{1 + LE \times \rho_l^{-1}/(PF \times pl \times \rho_p^{-1})}, \tag{13}$$

where LE is the lipid enrichment factor. For both experiments, D_0 is undetermined as are precise values for the parameters of the Saffman-Delbruck equation (1). Consequently, theoretical values of D_l/D_0, given by the low ϕ analytical expression, (11), are fit to the most dilute data points in both experiments to determine D_0.

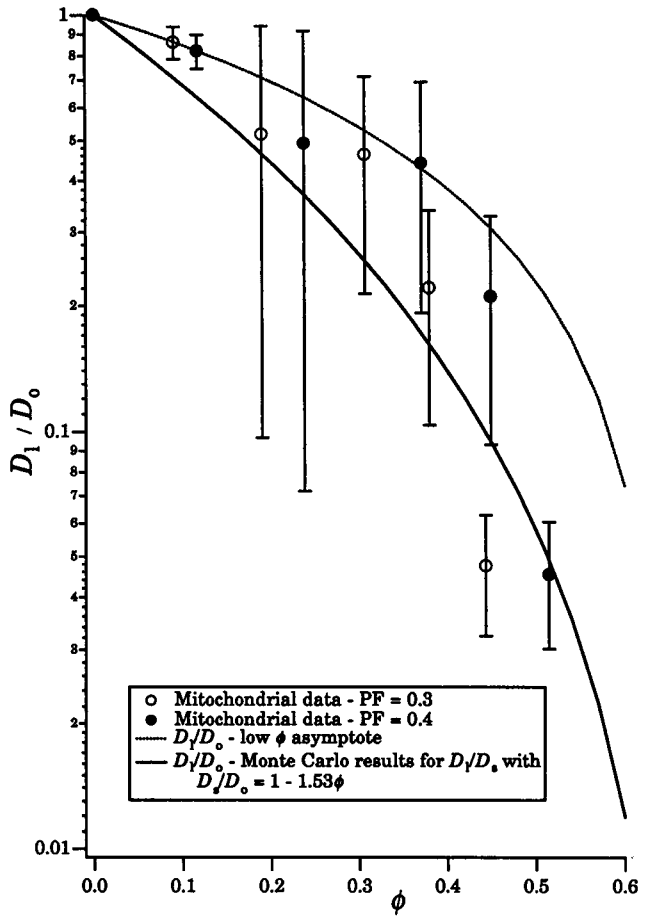

FIGURE 4 Comparison between theory and experiment for the diffusion of complex III in inner mitochondrial membranes enriched with soybean phospholipids. Again, the theoretical predictions fit the experimental data only when both thermodynamic and hydrodynamic interactions are included in the calculations. The low ϕ result is also shown for comparison and is similar in magnitude to the purely thermodynamic result that was shown in Fig. 3. The experimental data and error bars are interpreted from the results reported in Table II of Chazotte and Hackenbrock (1988). The results depend strongly on parameters used to determine experimental values for ϕ as demonstrated by the discrepancy between data generated with protein mass fractions (*PF*) in the membrane set to 0.3 or 0.4.

DISCUSSION AND CONCLUSIONS

Before we discuss the results in detail, we first comment on the experimental data. The experimental measurements of the diffusion coefficients of bacteriorhodopsin in reconstituted membranes were performed in multilamellar vesicles at *L/P* ratios as low as 30. Conceivably, the IMPs in adjacent bilayers could interact hydrodynamically. However, this would only occur if adjacent bilayers were separated by distances approximately equal to or less than the hydrodynamic screening length, $\lambda a \sim 500$ nm. If the bilayers are separated by more than λa, interactions are weak. In addition, bacteriorhodopsin is known to aggregate in its native bacterial purple membrane. Obviously, high levels of protein aggregation would significantly affect measured diffusion coefficients. Experiments indicate that only low levels of aggregation occur at *L/P* ratios of 40 or more (Cherry and Godfrey, 1981). The low level of aggregation that occurs at the lowest *L/P* ratios has only minor effects on D_0 and D_s for IMP diffusion coefficients because of the weak dependence of these diffusivities on the radii of IMPs (Saffman and Delbruck, 1975). Larger effects on D_1 may occur at high area fraction if noncircular protein aggregates display different hindering than circular individual proteins. Because the extent of aggregation and its effects on diffusivity appear minor and are ill-defined, we choose to analyze the results of these experiments without explicitly taking aggregation into account.

The experimental measurements of the diffusion coefficients of complex III in mitochondrial inner membranes occurred in a highly heterogeneous system. Inner mitochondrial membranes are composed of a large variety of IMPs and lipids. By assuming average properties for the IMPs and lipids, we neglect the influences of polydispersity on the hydrodynamics. For hydrodynamic interactions, polydispersity is probably a weak effect. Protein diffusivities vary weakly with protein radius a ($\ln a$ dependence). Provided the lipid molecules are smaller than the proteins such that the lipid remains a continuum fluid and there is no lipid phase separation induced by the heterogeneous lipid composition of the membrane, the only effect of lipid polydispersity would be to change the membrane viscosity. Until there is convincing evidence otherwise, we choose to use the simplest assumptions as a means to establish a basis for future comparisons.

Finally, diffusion data for gramicidin at various IMP concentrations are available (Tank et al., 1982), although we have chosen not to analyze them. Gramicidin is an unusually small IMP having a radius nearly equal to the radius of a lipid molecule. Hence, the fluid continuum model assumed in the derivation of D_s is not applicable. Free area theories would be better suited for the analysis of the concentration dependence of gramicidin diffusion (Scalettar and Abney, 1991).

As mentioned before, the results in Figs. 3 and 4 are most sensitive to assumptions that affect ϕ. Diffusion coefficients are strongly dependent on ϕ but have only a weak logarithmic dependence on λ. Accordingly, changes to the parameters from which ϕ are derived influence most strongly the comparison between theory and experiment. This can be seen in Fig. 4, where we have compared theoretical results with experimental data for complex III for values of *PF* equal to 0.3 and 0.4. Small changes in derived values for protein area fractions generate large differences in the quality of agreement between theory and experiment.

Keeping all these considerations in mind, there is good agreement between the theory that incorporates both thermodynamic and hydrodynamic interactions and experiment, as shown in Figs. 3 and 4. As expected, the theoretical asymptotic result for D_1, valid only at low ϕ and including only two body (hydrodynamic and thermodynamic) interactions, adequately matches the experimental long-time diffusivities at low ϕ, but is inadequate to explain the trend in the data at higher ϕ. Likewise, a theory that excludes hydrodynamics and includes multibody thermodynamics also overpredicts the diffusivity (Fig. 3) to the same extent. Because the

decrease in diffusivity with increasing ϕ appears to be quantitatively similar in solely hydrodynamic or thermodynamic theories (Fig. 3), both types of interactions appear to contribute equally to the low diffusivities at higher ϕ.

The close correspondence between our theoretical calculations and published experimental results at high ϕ needs to be studied further. The result for D_s given in (2) is a low ϕ asymptote, yet we have used this result as the reference diffusion coefficient to determine D_l absolutely at all ϕ. There are two possibilities for the close correspondence at high ϕ between experimental data and theoretical predictions made using both Eq. 4 and the low ϕ asymptote for D_s. It could occur because errors in the theoretical values of D_s extrapolated from the low ϕ asymptote are cancelled by effects generated at high ϕ for the calculation of D_l/D_s (Eq. 4). However, this possibility is contrary to Rallison's reasoning, which suggests that the results for D_l/D_s given by (4) and (6) are precise at high ϕ because D_l/D_s is determined primarily by multibody thermodynamic interactions. Alternatively, the close correspondence could occur because higher order, multiparticle hydrodynamic effects either are insignificant or cancel for short time diffusion coefficients. This issue, however, can only be fully resolved by more encompassing numerical procedures such as Stokesian dynamics simulations (Brady and Bossis, 1988).

Nevertheless, we believe that these studies show that both hydrodynamic and thermodynamic interactions are important determinants of D_l at high area fractions. They appear to be equal determinants, because D_l/D_s from thermodynamic calculations and the low ϕ asymptote for D_l/D_0 (largely a hydrodynamic result) are similar functions of ϕ (see Fig. 3). Our results make an important step toward explaining the differences that exist between experimental results and theoretical predictions based solely on thermodynamic interactions for the diffusion of IMPs in lipid bilayer membranes (Saxton, 1987; Scalettar and Abney, 1991).

If, as we believe, hydrodynamic interactions play an important role in protein diffusion in lipid bilayers, experimentalists should be aware that hydrodynamic variables such as membrane and aqueous phase viscosities are critical determinants of diffusion rates and should be measured independently and altered when possible. Measurements of viscosity must be done in dilute suspensions to avoid measuring effective viscosities, which are functions of protein concentration. Also, further experimental investigations of protein diffusion coefficients in reconstituted systems using large unilamellar vesicles containing a single lipid and a single nonaggregating IMP species are needed to compare rigorously with the hydrodynamic theory. The data for neither the diffusion of bacteriorhodopsin (because of multilayer blebs) nor complex III (because of lipid and protein heterogeneity) are ideal for testing the theoretical predictions.

The results presented in this paper do not explain the low diffusion coefficients observed in plasma membranes in which a large fraction of the IMPs are immobile (Henis and Elson, 1981). As we demonstrate in the companion paper (Bussell et al., 1995), the hydrodynamic interactions in plasma membranes are different than those in lipid bilayers. Explicit consideration of the proper hydrodynamic interactions in plasma membranes leads naturally to a theory that predicts the low IMP diffusion coefficients observed in plasma membranes.

This work was supported by the National Science Foundation in the form of a Creativity Award (EID-8710373) to S. J. Bussell and a Presidential Young Investigator Award (BCS-8958632) to D. A. Hammer.

REFERENCES

Abney, J. R., B. A. Scalettar, and J. C. Owicki. 1989a. Self-diffusion of interacting membrane proteins. *Biophys. J.* 55:817–833.

Abney, J. R., B. A. Scalettar, and J. C. Owicki. 1989b. Mutual diffusion of interacting membrane proteins. *Biophys. J.* 56:315–326.

Axelrod, D., D. E. Koppel, J. Schlessinger, E. Elson, and W. W. Webb. 1976. Mobility measurements by analysis of fluorescence photobleaching recovery kinetics. *Biophys. J.* 16:1055–1069.

Brady, J. F., and G. Bossis. 1988. Stokesian dynamics. *Annu. Rev. Fluid Mech.* 20:111–157.

Bussell, S. J. 1992. Hydrodynamics, diffusion, and diffusion-limited reaction of integral membrane proteins. Ph.D. Thesis, Cornell University, Ithaca, NY.

Bussell, S. J., D. L. Koch, and D. A. Hammer. 1992. The resistivity and mobility functions for a model system of two equal-sized proteins in a lipid bilayer. *J. Fluid Mech.* 243:679–697.

Bussell, S. J., D. A. Hammer, and D. L. Koch. 1994. The effect of hydrodynamic interactions on the tracer and gradient diffusion of integral membrane proteins in lipid bilayers. *J. Fluid Mech.* 258:167–190.

Bussell, S. J., D. L. Koch, and D. A. Hammer. 1995. The effect of hydrodynamic interactions on the diffusion of integral membrane proteins: diffusion in plasma membranes. *Biophys. J.* 68:1836–1849.

Chazotte, B., and C. R. Hackenbrock. 1988. The multicollisional, obstructed, long-range diffusional nature of mitochondrial electron transport. *J. Biol. Chem.* 263:14359–14367.

Cherry, R. J., and R. E. Godfrey. 1981. Anisotropic rotation of bacteriorhodopsin in lipid membranes. *Biophys. J.* 36:257–276.

Deatherage, J. F., R. Henderson, and R. A. Capaldi. 1982. Relationship between membrane and cytoplasmic domains in cytochrome *c* oxidase by electron microscopy in media of different density. *J. Mol. Biol.* 158: 501–514.

Edidin, M. 1987. Rotational and lateral diffusion of membrane proteins and lipids: phenomena and function. *Curr. Top. Membr. Trans.* 29:91–127.

Gennis, R. B. 1989. Biomembranes: Molecular Structure and Function. Springer Verlag, New York.

Henderson, R., and P. N. T. Unwin. 1975. Three-dimensional model of purple membrane obtained by electron microscopy. *Nature.* 257:28–32.

Henis, Y. I., and E. L. Elson. 1981. Inhibition of the mobility of mouse lymphocyte surface immunoglobulins by locally bound concanavalin A. *Proc. Natl. Acad. Sci. USA.* 78:1072–1076.

Leonard, K., H. Haiker, and H. Weiss. 1987. Three-dimensional structure of NADH: ubiquinone reductase (complex I) from *Neurospora* mitochondria determined by electron microscopy of membrane crystals. *J. Mol. Biol.* 194:277–286.

Medina-Noyala, M. 1988. Long-time self diffusion in concentrated colloidal dispersions. *Phys. Rev. Lett.* 60:2705–2708.

Minton, A. P. 1989. Lateral diffusion of membrane proteins in protein-rich membranes. A simple, hard-core model for the concentration dependence of the two-dimensional diffusion coefficient. *Biophys. J.* 55: 805–808.

Peters, R., and R. J. Cherry. 1982. Lateral and rotational diffusion of bacteriorhodopsin in lipid bilayers: experimental test of the Saffman-Delbruck equations. *Proc. Natl. Acad. Sci. USA.* 79:4317–4321.

Pink, D. A. 1985. Protein lateral movement in lipid bilayers. Simulation studies of its dependence upon protein concentration *Biochim. Biophys. Acta.* 818:200–204.

Rallison, J. M. 1988. Brownian diffusion in concentrated suspensions of interacting particles. *J. Fluid Mech.* 186:471–500.

Russel, W. B., and A. P. Gast. 1986. Nonequilibrium statistical mechanics of concentrated colloidal dispersions: hard spheres in weak flows. *J. Chem. Phys.* 84:1815–1826.

Saffman, P. G., and M. Delbruck. 1975. Brownian motion in Biological membranes. *Proc. Natl. Acad. Sci. USA.* 72:3111–3113.

Saxton, M. J. 1987. Lateral diffusion in an archipelago: the effect of mobile obstacles. *Biophys. J.* 52:989–997.

Scalettar, B. A., and J. R. Abney. 1991. Molecular crowding and protein diffusion in biological membranes. *Comments Mol. Cell. Biophys.* 7: 79–107.

Singer, S. J., and G. L. Nicolson. 1972. The fluid mosaic model of the structure of cell membranes. *Science.* 175:720–731.

Tank, D. W., E. S. Wu, P. R. Meers, and W. W. Webb. 1982. Lateral diffusion of gramicidin c in phospholipid multibilayers: effects of cholesterol and high gramicidin concentration. *Biophys. J.* 40: 129–135.

Tank, D. W., E. S. Wu, and W. W. Webb. 1982. Enhanced molecular diffusibility in muscle membrane blebs: release of lateral constraints. *J. Cell Biol.* 92:207–212.

Wu, E. S., D. W. Tank, and W. W. Webb. 1982. Unconstrained lateral diffusion of concanavalin A receptors on bulbous lymphocytes. *Proc. Natl. Acad. Sci. USA.* 79:4962–4966.